NACA

RESEARCH MEMORANDUM

AERODYNAMIC CHARACTERISTICS OF TWO PLANE, UNSWEPT

TAPERED WINGS OF ASPECT RATIO 3 AND 3-PERCENT

THICKNESS FROM TESTS ON A TRANSONIC BUMP

By Horace F. Emerson and Bernard M. Gale

Ames Aeronautical Laboratory
Moffett Field, Calif.

NATIONAL ADVISORY COMMITTEE
FOR AERONAUTICS
WASHINGTON
May 2, 1952

NATIONAL ADVISORY COMMITTEE FOR AERONAUTICS

RESEARCH MEMORANDUM

AERODYNAMIC CHARACTERISTICS OF TWO PLANE, UNSWEPT

TAPERED WINGS OF ASPECT RATIO 3 AND 3-PERCENT

THICKNESS FROM TESTS ON A TRANSONIC BUMP

By Horace F. Emerson and Bernard M. Gale

SUMMARY

An investigation was conducted in the Ames 16-foot high-speed wind tunnel using the transonic bump technique to determine the aerodynamic characteristics of two unswept tapered wings through the transonic speed range. The Mach number range was 0.60 to 1.10 and the Reynolds number range was 1.9 million to 2.5 million. Each wing had a taper ratio of 0.39, an aspect ratio of 3.0, and the 60-percent-chord line unswept. One of the wings utilized the NACA 0003-63 section, while the other had a 3-percent-thick, circular-arc section. Lift, drag, and pitching-moment data are presented for both wings with and without surface roughness over the first 10 percent of the chord. The round-nose airfoil had slightly better aerodynamic characteristics at Mach numbers less than 1.0.

The wing having the circular-arc section had been previously tested in combination with a body in the Ames 6- by 6-foot supersonic wind tunnel at both subsonic and supersonic Mach numbers, and the results are presented herein.

INTRODUCTION

The Ames Aeronautical Laboratory has in progress an experimental investigation of the aerodynamic characteristics of wings of interest in the design of high-speed fighter aircraft. This program included an investigation in the Ames 6- by 6-foot supersonic wind tunnel at both subsonic and supersonic Mach numbers of a wing-body combination having a 3-percent-thick, unswept, tapered wing with circular-arc sections and an aspect ratio of 3.1 (reference 1).

In order to obtain data through the near-sonic speed range, a similar wing of aspect ratio 3.0 having a 3-percent-thick, circular-arc section was investigated in the Ames 16-foot high-speed wind tunnel on the transonic bump. A wing with identical plan form but having the NACA 0003-63 section was also tested to provide comparative data for a wing with a round-nose section.

NOTATION

C_D drag coefficient $\left(\dfrac{\text{twice semispan drag}}{qS}\right)$

C_L lift coefficient $\left(\dfrac{\text{twice semispan lift}}{qS}\right)$

C_m pitching-moment coefficient, referred to $0.25\bar{c}$
$\left(\dfrac{\text{twice semispan pitching moment}}{qS\bar{c}}\right)$

A aspect ratio $\left(\dfrac{b^2}{S}\right)$

$\dfrac{L}{D}$ lift-drag ratio

$\left(\dfrac{L}{D}\right)_{max}$ maximum lift-drag ratio

M Mach number

R Reynolds number based on mean aerodynamic chord

S total wing area (twice wing area of semispan model), square feet

V velocity, feet per second

b twice span of semispan model, feet

c local chord, feet

$\bar{c}$ mean aerodynamic chord $\left(\dfrac{\int_0^{b/2} c^2 dy}{\int_0^{b/2} c\ dy}\right)$, feet

q dynamic pressure $\left(\dfrac{1}{2}\rho V^2\right)$, pounds per square foot

y spanwise distance from plane of symmetry, feet

α angle of attack, degrees

ρ air density, slugs per cubic foot

$\dfrac{dC_L}{d\alpha}$ slope of lift curve measured at zero lift, per degree

$\dfrac{dC_m}{dC_L}$ slope of pitching-moment curve measured at zero lift

APPARATUS AND MODELS

The models were tested on a transonic bump in the Ames 16-foot high-speed wind tunnel. A description of the bump may be found in reference 2. Aerodynamic forces and moments were measured by means of an electrical strain-gage balance mounted inside the bump.

The two 16-foot-tunnel models were identical in plan form, having an unswept 60-percent-chord line, an aspect ratio of 3.0, and a taper ratio of 0.39, but differed in streamwise section; one employed a circular-arc section and the other the NACA 0003-63 section. Figure 1 is a photograph of one of the models mounted on the 16-foot bump, and a two-view drawing of the model having the 3-percent-thick, symmetrical, circular-arc section is presented as figure 2. A fence located 3/16 inch from the bump surface was used to reduce the effects of leakage which resulted from clearance required between the wing and bump surface. The ratio of fence area to semispan wing area was 0.434.

TESTS AND PROCEDURE

The aerodynamic characteristics of the wings were investigated over a Mach number range from 0.60 to 1.10. The variation of test Reynolds number with Mach number is shown in figure 3. The angle-of-attack range extended from -6° to the stall, or to an angle limited by the capacity of the strain-gage balance. For some of the tests surface roughness was added by scattering No. 60 carborundum grit in sufficient quantity to cover approximately 15 percent of the area forward of the 10-percent-chord stations on both the upper and lower surfaces.

Figure 4 shows typical Mach number contours of the flow over the bump superposed on the outline of the wings to indicate the Mach number variation over the test region. The test Mach numbers presented in this

report were taken to be the Mach number of the contour passing through the 25-percent point of the mean aerodynamic chord.

The test data have been reduced to standard NACA coefficients. The drag data were corrected to account for an interaction between the lift and drag components of the balance. A tare-drag coefficient, evaluated by testing a fence alone, was found to be 0.0020 and was essentially independent of Mach number and angle of attack. Interference effects of the fence and effects of leakage around the fence are not known and no corrections for these effects have been made. An angle-of-attack correction of -0.4° was included to account for the cross flow over the bump.

RESULTS AND DISCUSSION

Figures 5 and 6 present force and moment data for the wing models having the circular-arc and the NACA 0003-63 sections, respectively. Figure 7 presents the variations of several aerodynamic characteristics with Mach number for both wings where the slope parameters have been determined at zero lift. Figures 5 and 7 also include data obtained in the Ames 6- by 6-foot wind tunnel at a Reynolds number of 2.4 million (reference 1).

Figures 5(a) and 6(a) show the variation of lift coefficient with angle of attack for the models with the circular-arc section and the NACA 0003-63 section, respectively. As may be seen in figure 7(a), the lift-curve slope of the NACA 0003-63 airfoil is higher than that of the circular-arc airfoil.

Figures 5(b) and 6(b) present drag coefficients for the models. Data obtained with surface roughness applied to the wing indicate somewhat higher drag, but surface roughness did not otherwise materially affect the aerodynamic characteristics of the wing models. Figure 7(b) presents drag coefficient as a function of Mach number and indicates some advantage for the wing with the NACA 0003-63 section over the wing with the circular-arc section in the subsonic Mach number range.

Figures 5(c) and 6(c) present the variation of pitching-moment coefficient with lift coefficient for the models. The pitching-moment data from the 6- by 6-foot tunnel have been transferred to the 25-percent point of the mean aerodynamic chord. The data obtained in the 6- by 6-foot tunnel show a less stable trend than those obtained in the 16-foot tunnel which can be attributed to the destabilizing effect of the body. Reference 3 presents data from the 6- by 6-foot tunnel which, when used in conjuntion with data from reference 1, indicate that about 60 percent of the difference between the moment curves from the two facilities is due to the presence of the body. Probably a large part of the remaining difference is the result of wing-body interference.

Figure 7(c) presents the variation of pitching-moment coefficient with Mach number and indicates an abrupt stability change between Mach numbers of 0.90 and 1.10 for both the model having the NACA 0003-63 section and the model with the circular-arc section. It can be seen that the stability variation for the wing with the NACA 0003-63 section was not as large as that for the wing with the circular-arc section.

Figures 5(d) and 6(d) present the variation of lift-drag ratio with lift coefficient for the models. Figures 7(d) and 7(e) show the variation of maximum lift-drag ratio with Mach number and the variation of lift coefficient at maximum lift-drag ratio with Mach number, respectively. The model having the NACA 0003-63 section attained higher values of maximum lift-drag ratio between Mach numbers of 0.60 and 0.90 than did the model with the circular-arc section.

CONCLUDING REMARKS

Of the two wings investigated in the 16-foot wind tunnel, the model with the NACA 0003-63 airfoil showed some advantage over the circular-arc airfoil in the subsonic Mach number range. The wing with the rounded leading edge had a higher lift-curve slope, not as large a stability variation, a somewhat higher maximum lift-drag ratio, and a slightly lower drag up to a Mach number of at least 0.90.

Ames Aeronautical Laboratory,
National Advisory Committee for Aeronautics,
Moffett Field, Calif.

REFERENCES

1. Reese, David E., and Phelps, E. Ray: Lift, Drag, and Pitching Moment of Low-Aspect-Ratio Wings at Subsonic and Supersonic Speeds - Plane Tapered Wing of Aspect Ratio 3.1 With 3-Percent-Thick, Biconvex Section. NACA RM A50K28, 1951.

2. Axelson, John A., and Taylor, Robert A.: Preliminary Investigation of the Transonic Characteristics of an NACA Submerged Inlet. NACA RM A50C13, 1950.

3. Heitmeyer, John C.: Lift, Drag, and Pitching Moment of Low-Aspect-Ratio Wings at Subsonic and Supersonic Speeds - Body of Revolution. NACA RM A51H22, 1951.
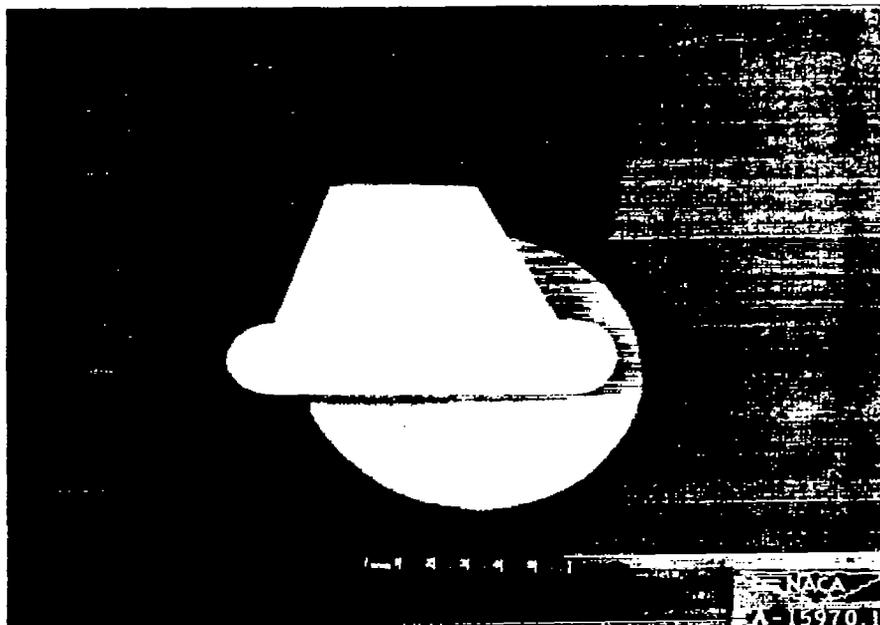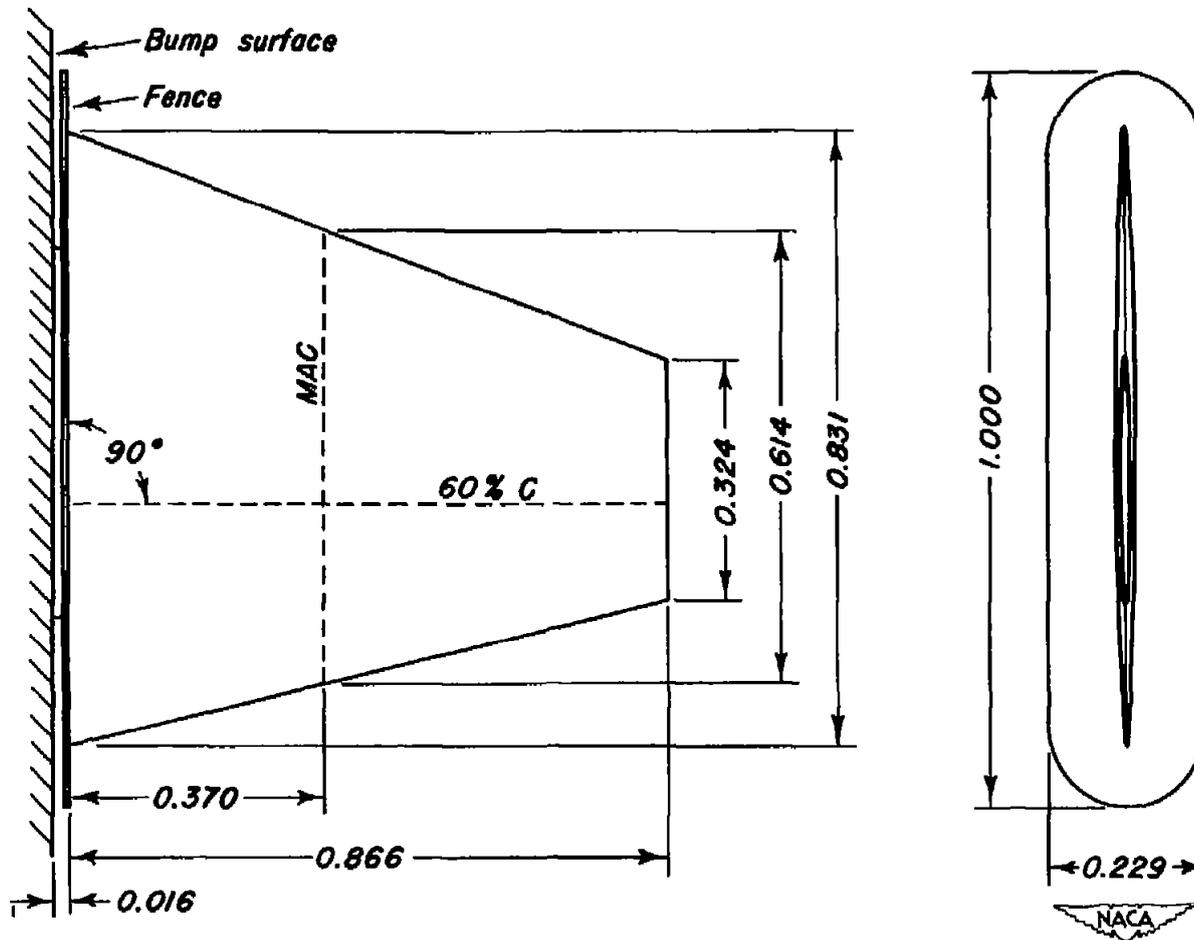
Figure 1.— Photograph of one of the models mounted on the 16-foot
high-speed wind-tunnel bump.

Bump surface

Fence

90°

MAC

60% C

0.324

0.614

0.831

0.370

0.866

0.016

1.000

0.229

All dimensions shown in feet

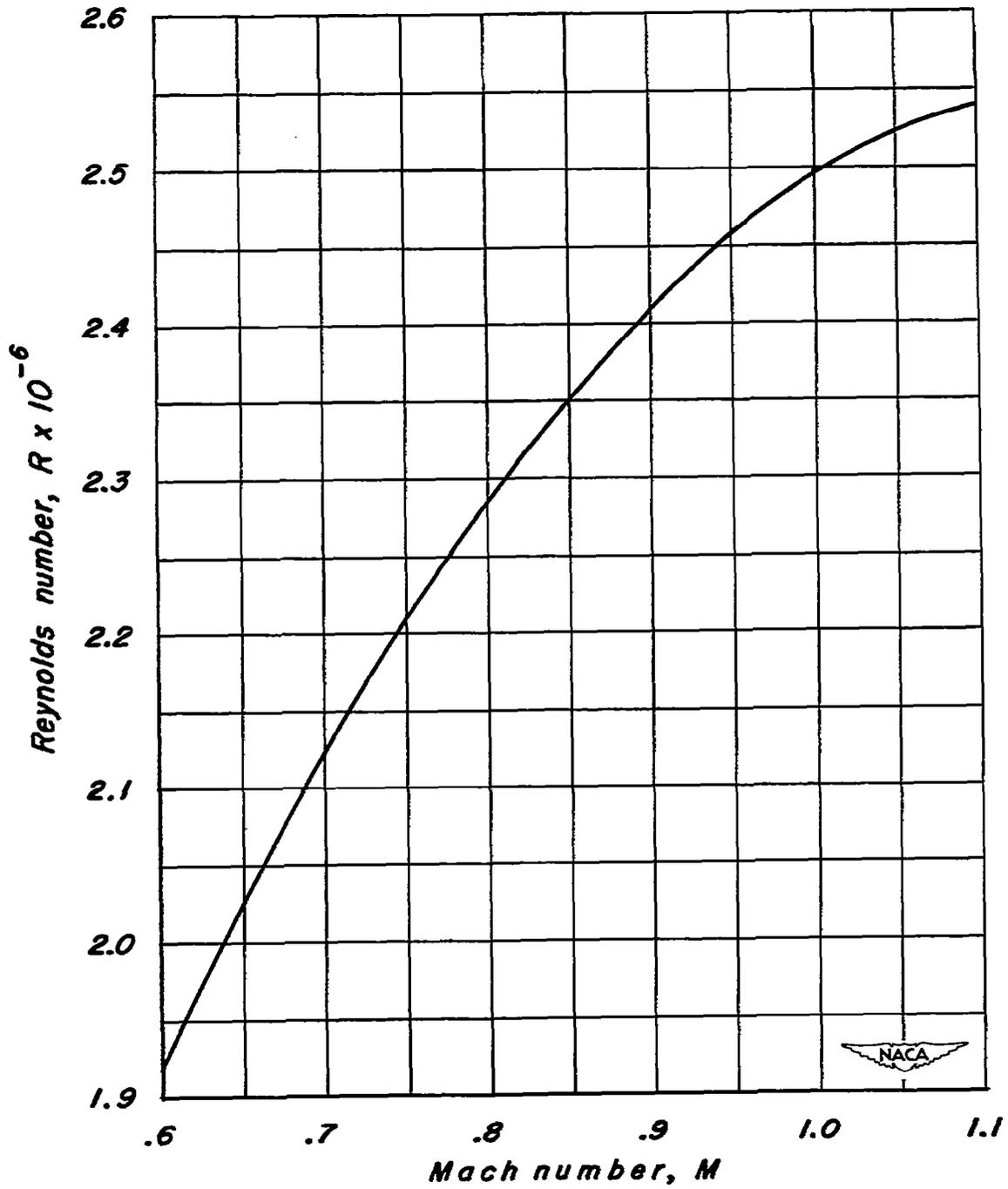Figure 2.—A two-view drawing of the wing model having the 3-percent-thick circular-arc section.

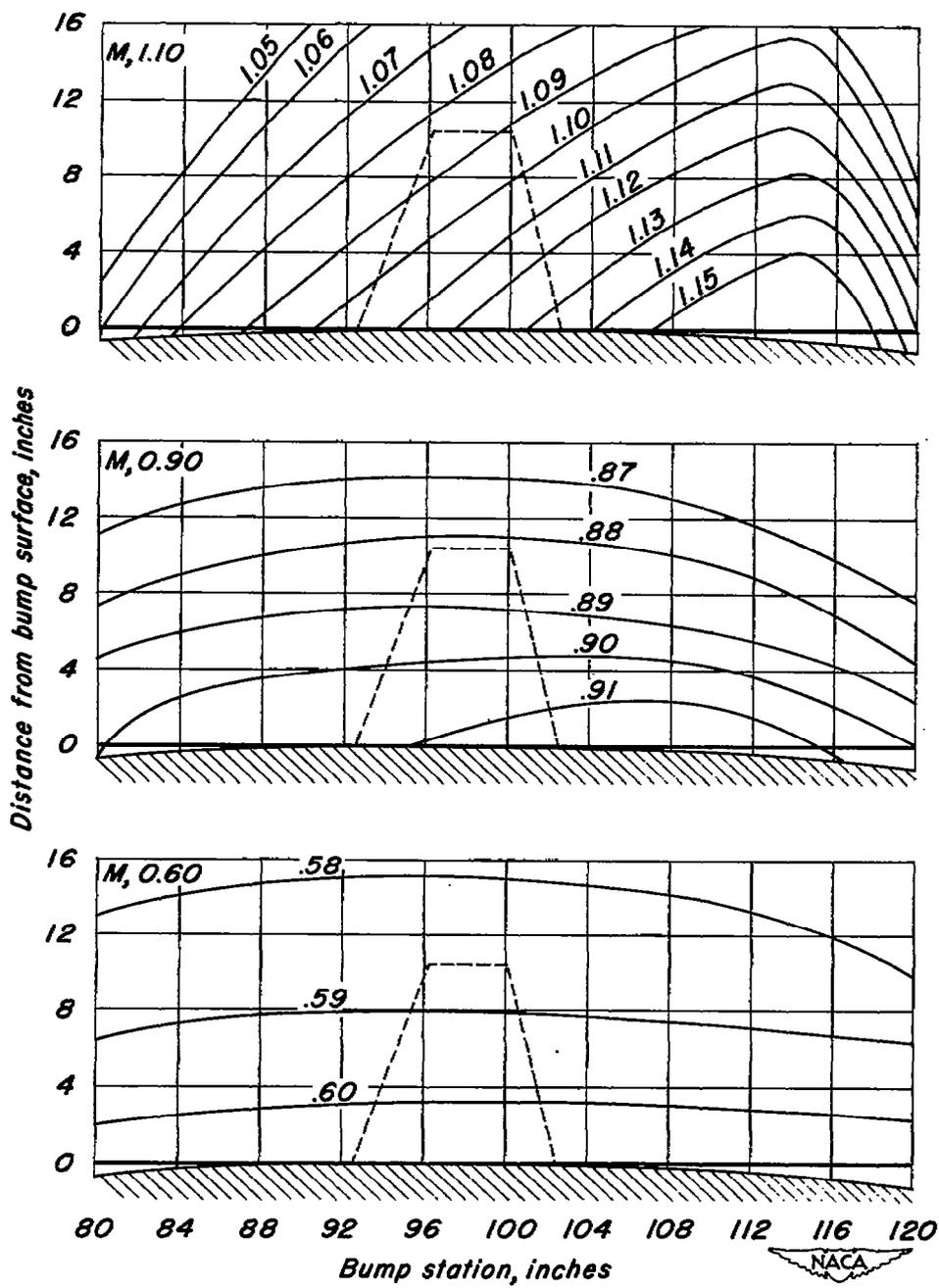Figure 3.—Variation of Reynolds number with Mach number.

Figure 4.- Typical Mach number contours over the transonic bump
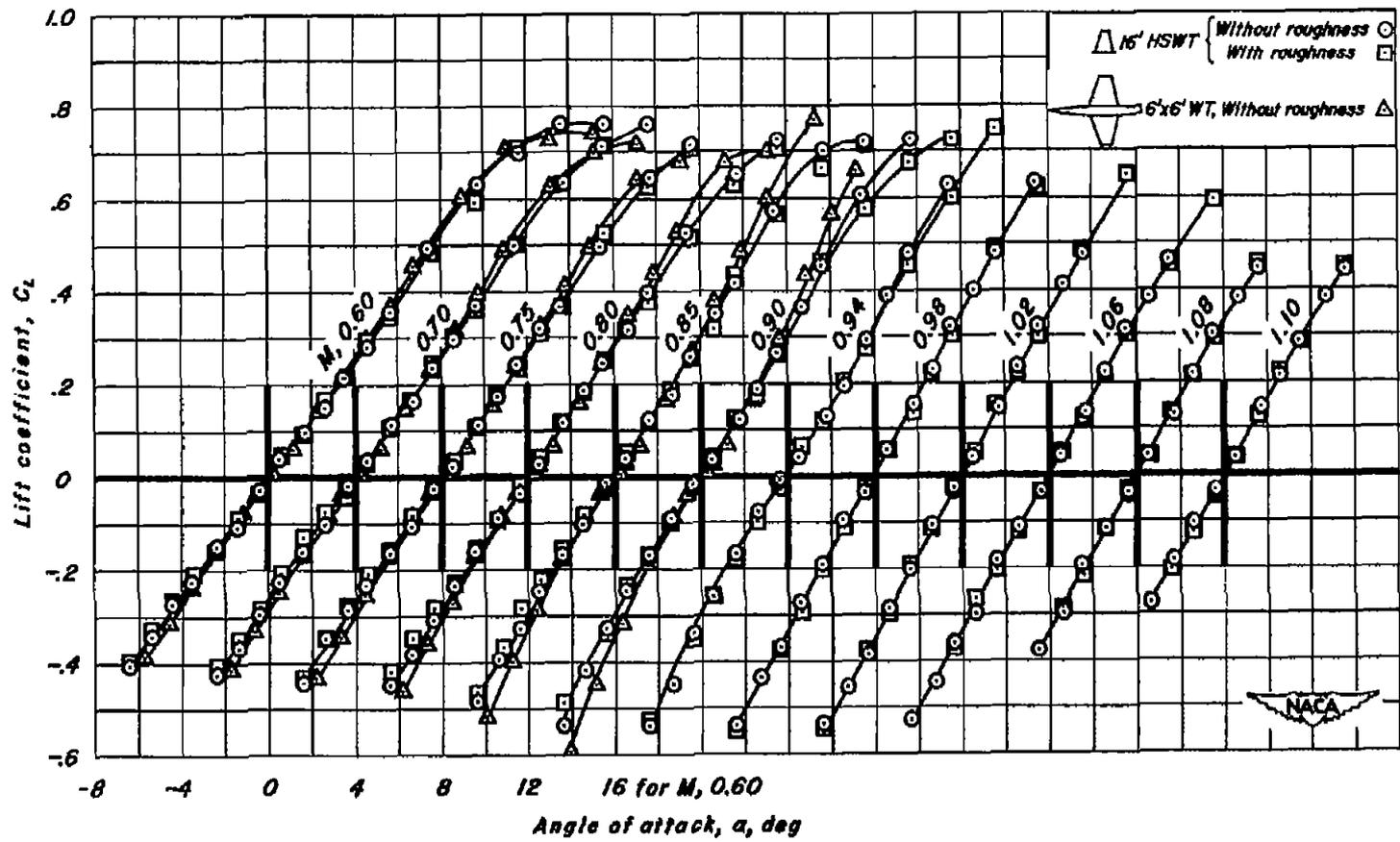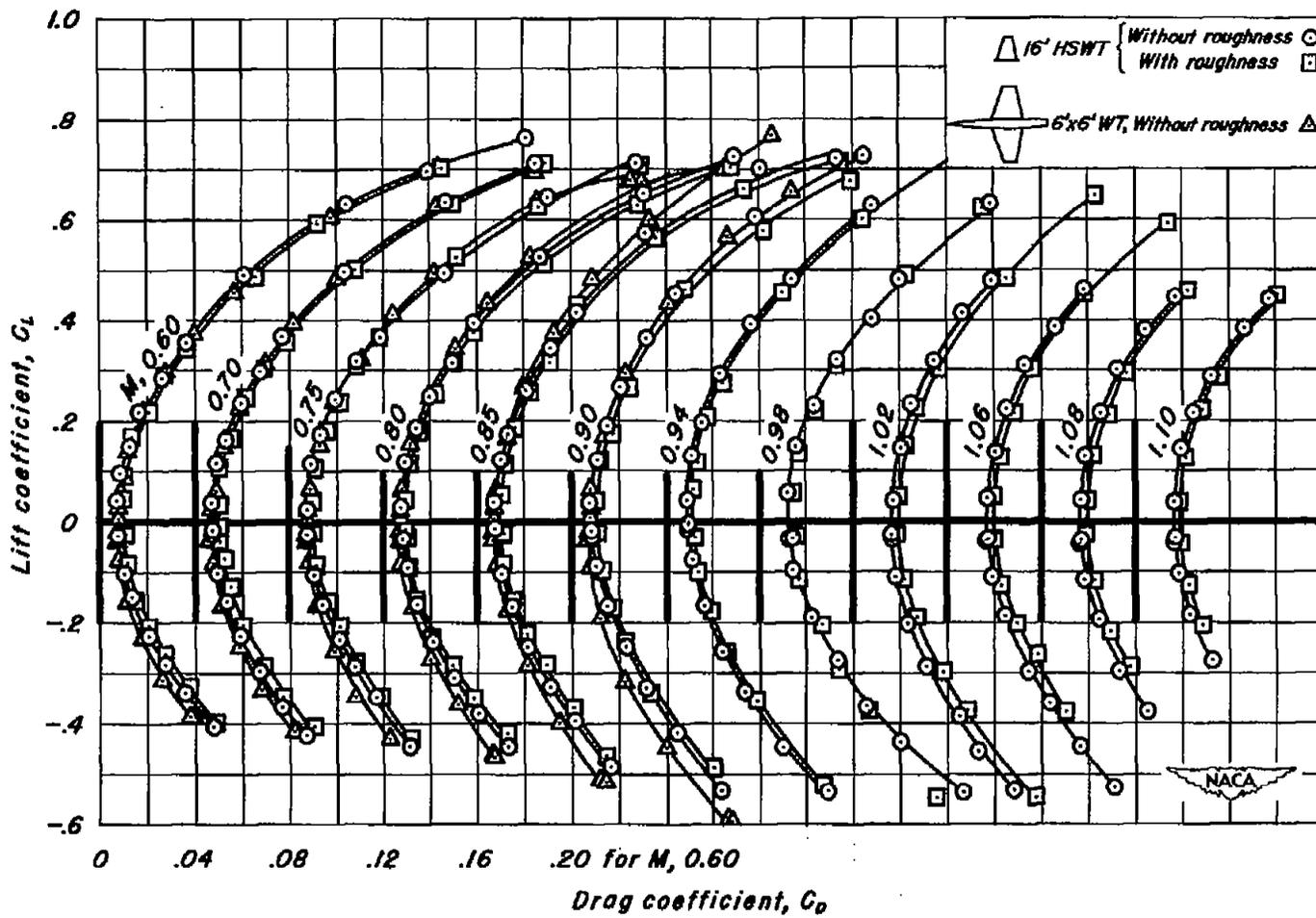in the Ames 16-foot high-speed wind tunnel.

(a) C_L vs a

Figure 5.—The aerodynamic characteristics of the wing having the 3-percent-thick circular-arc section.

(b) C_L vs C_D

Figure 5.- Continued.
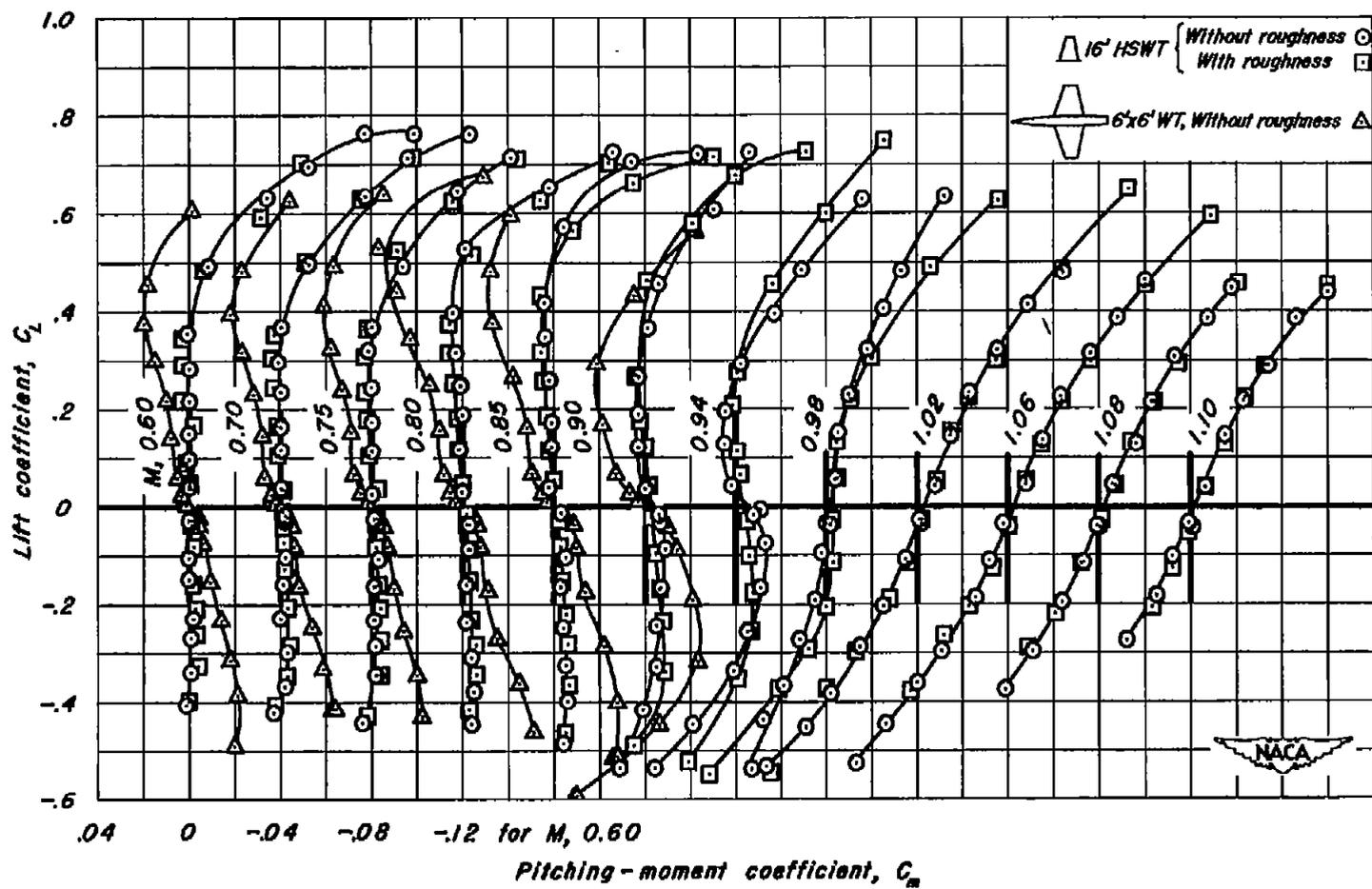
(c) C_L vs C_m

Figure 5.- Continued.
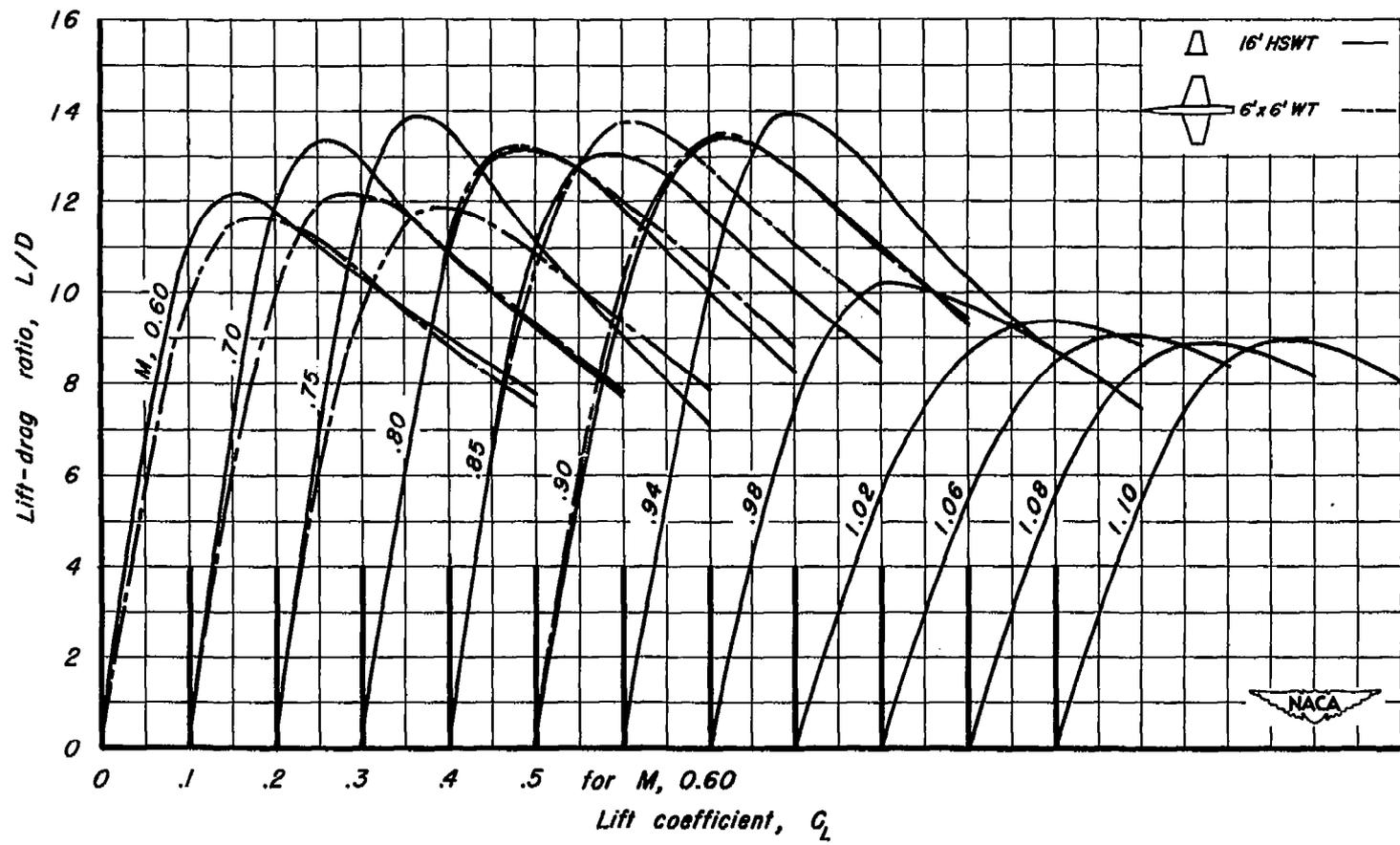
(d) L/D vs C_L

Figure 5.- Concluded.
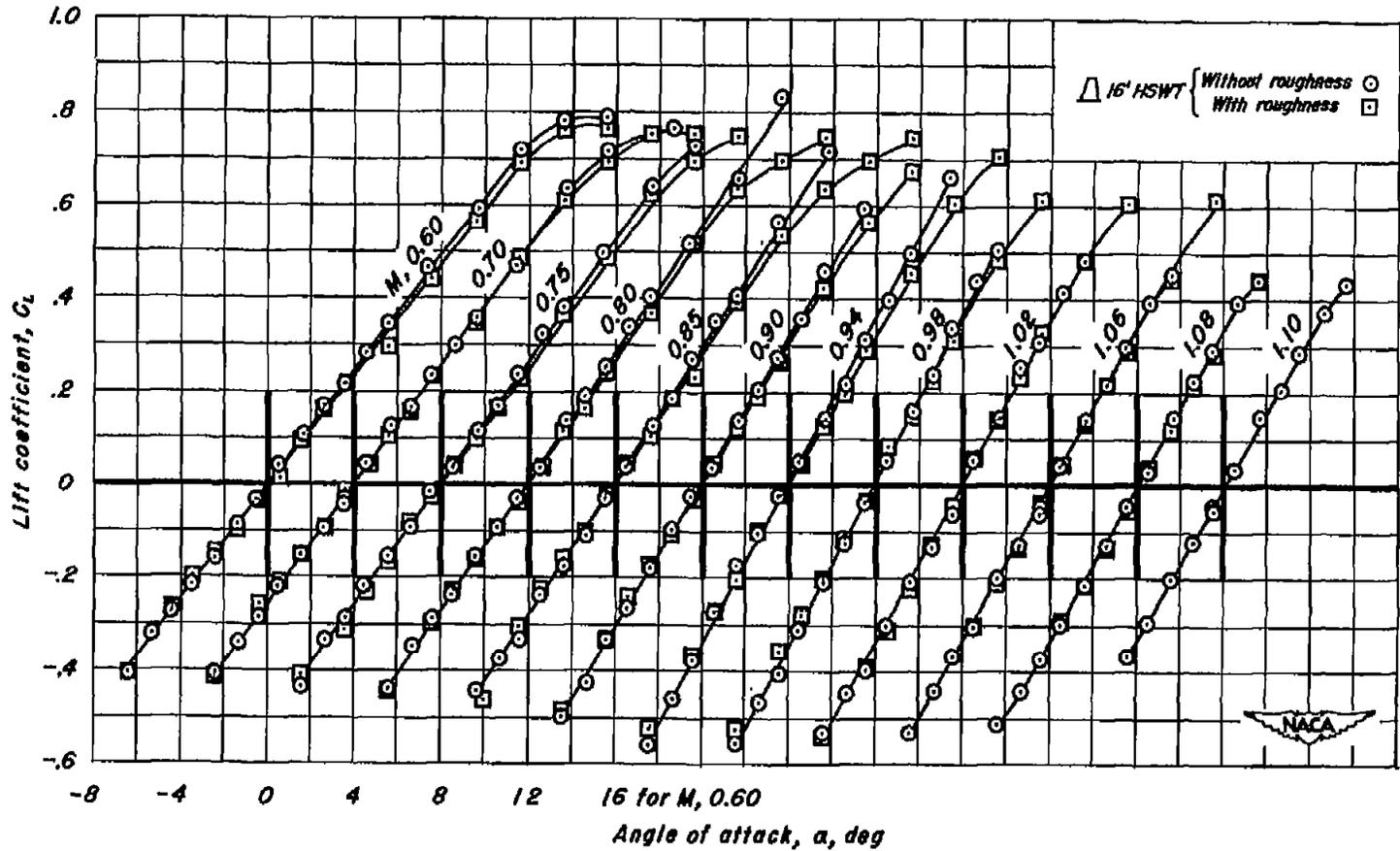
(a) C_L vs α

Figure 6.—The aerodynamic characteristics of the wing having the NACA 0003-63 section.
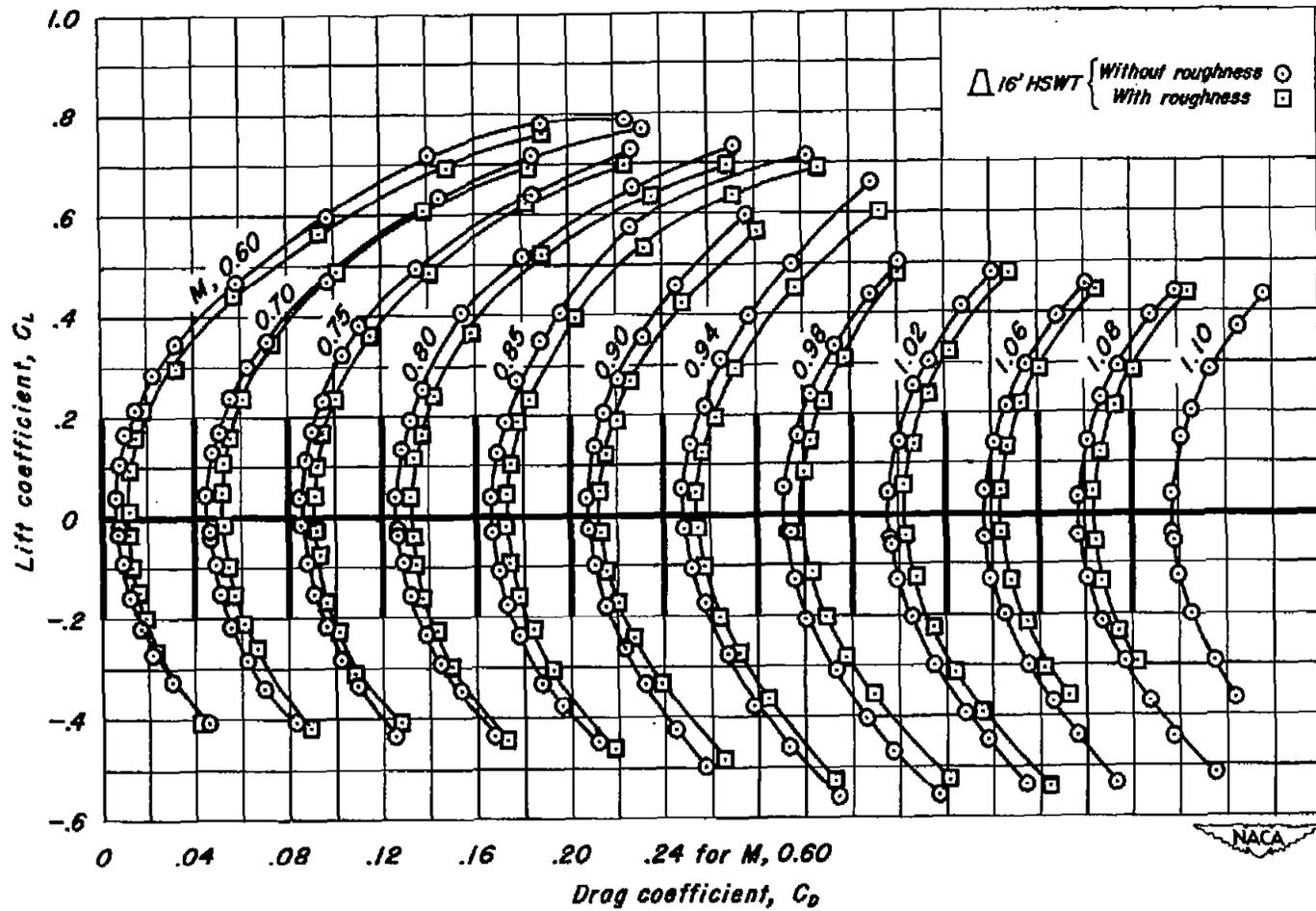
(b) C_L vs C_D

Figure 6.- Continued.
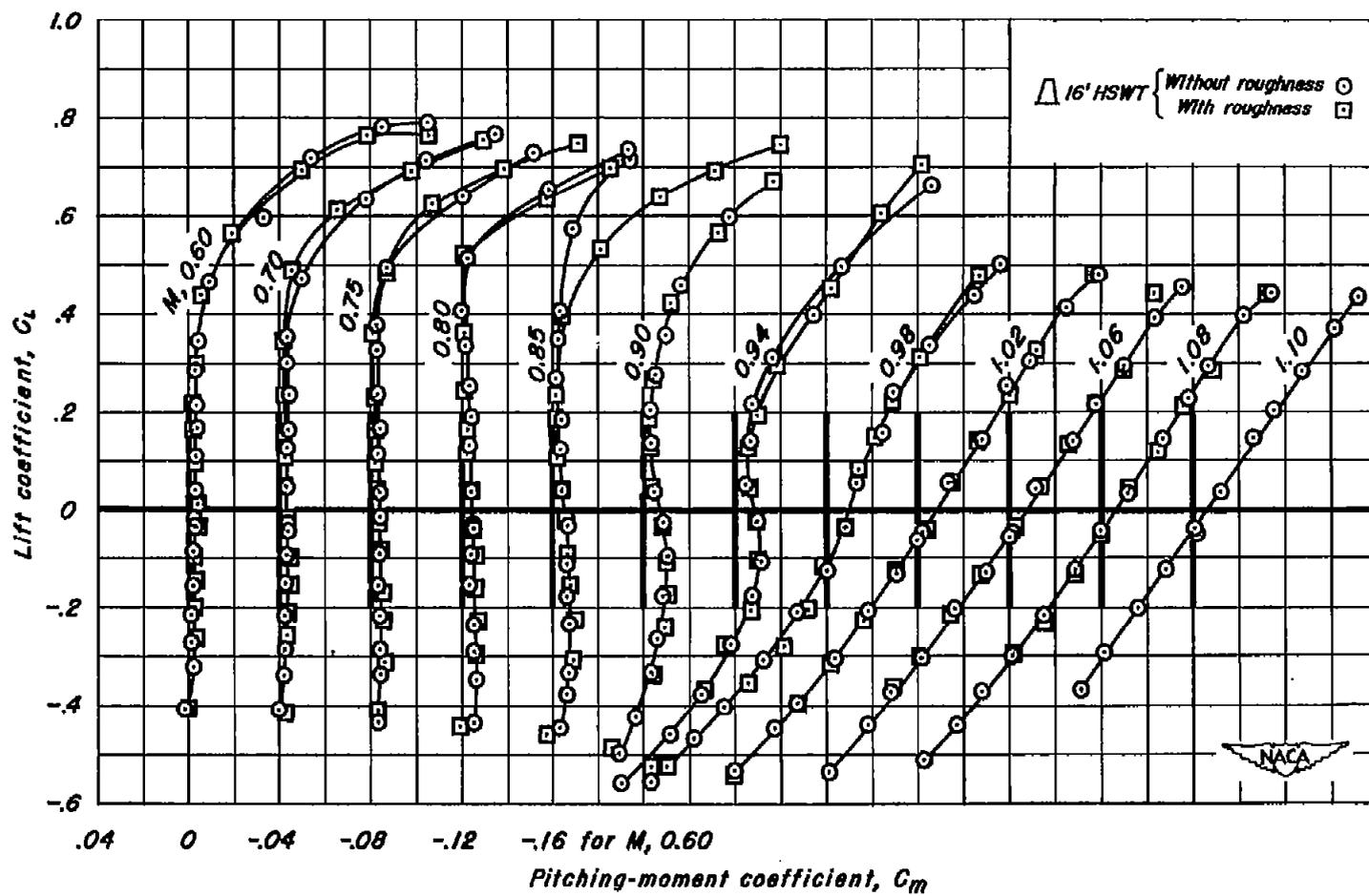
(c) C_L vs C_m

Figure 6.- Continued.
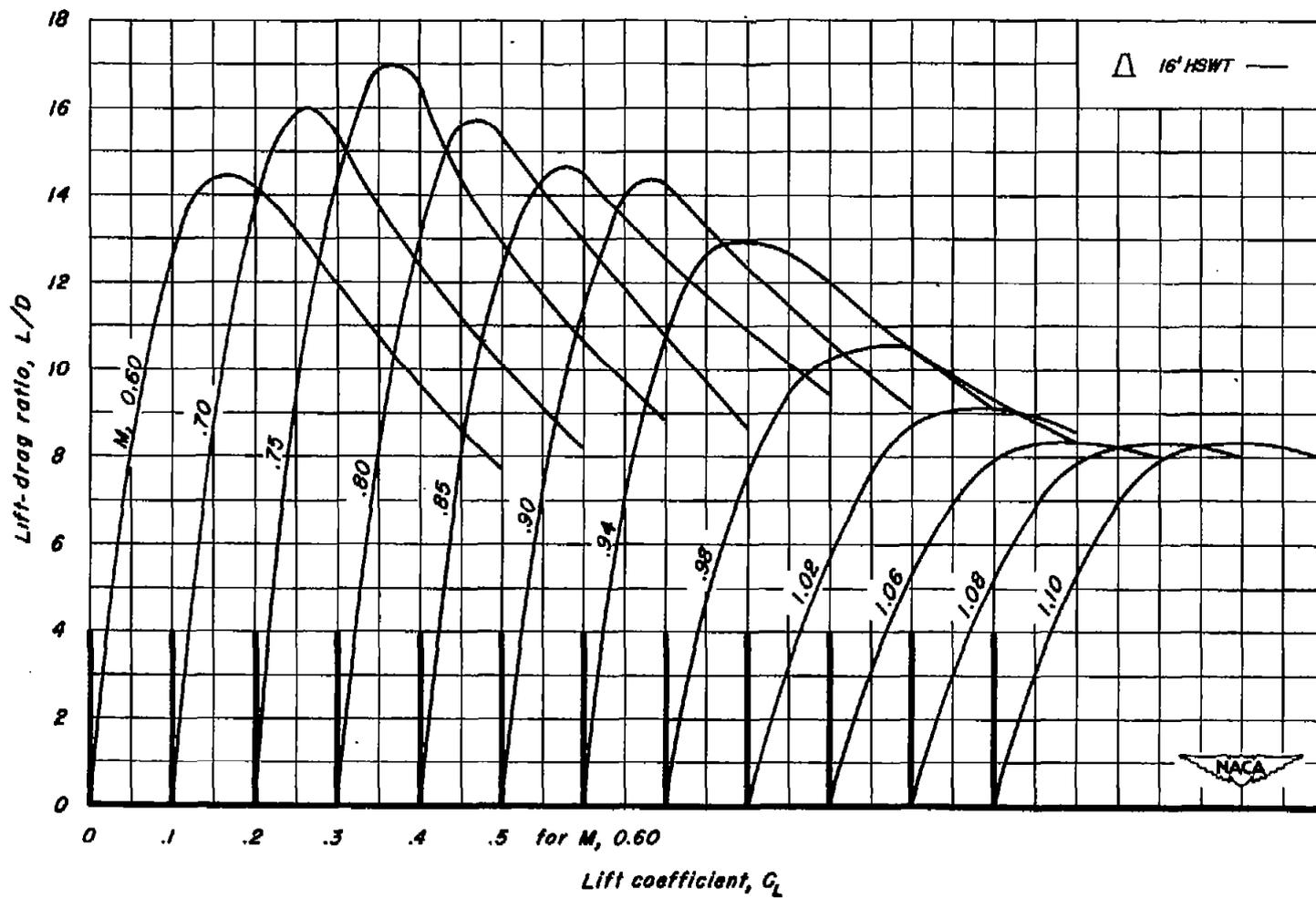
(d) L/D vs C_L

Figure 6.- Concluded.
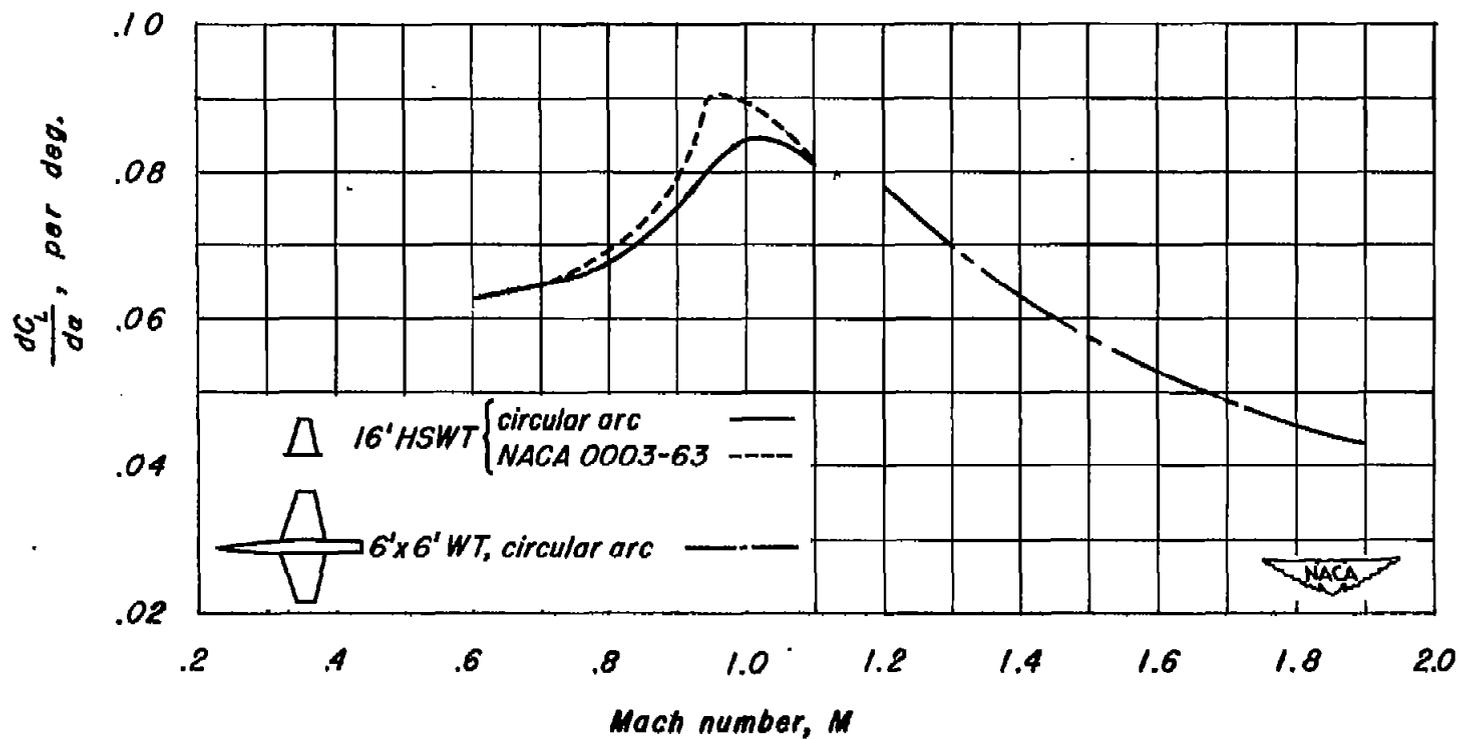
(a) $\dfrac{dC_L}{da}$ vs M

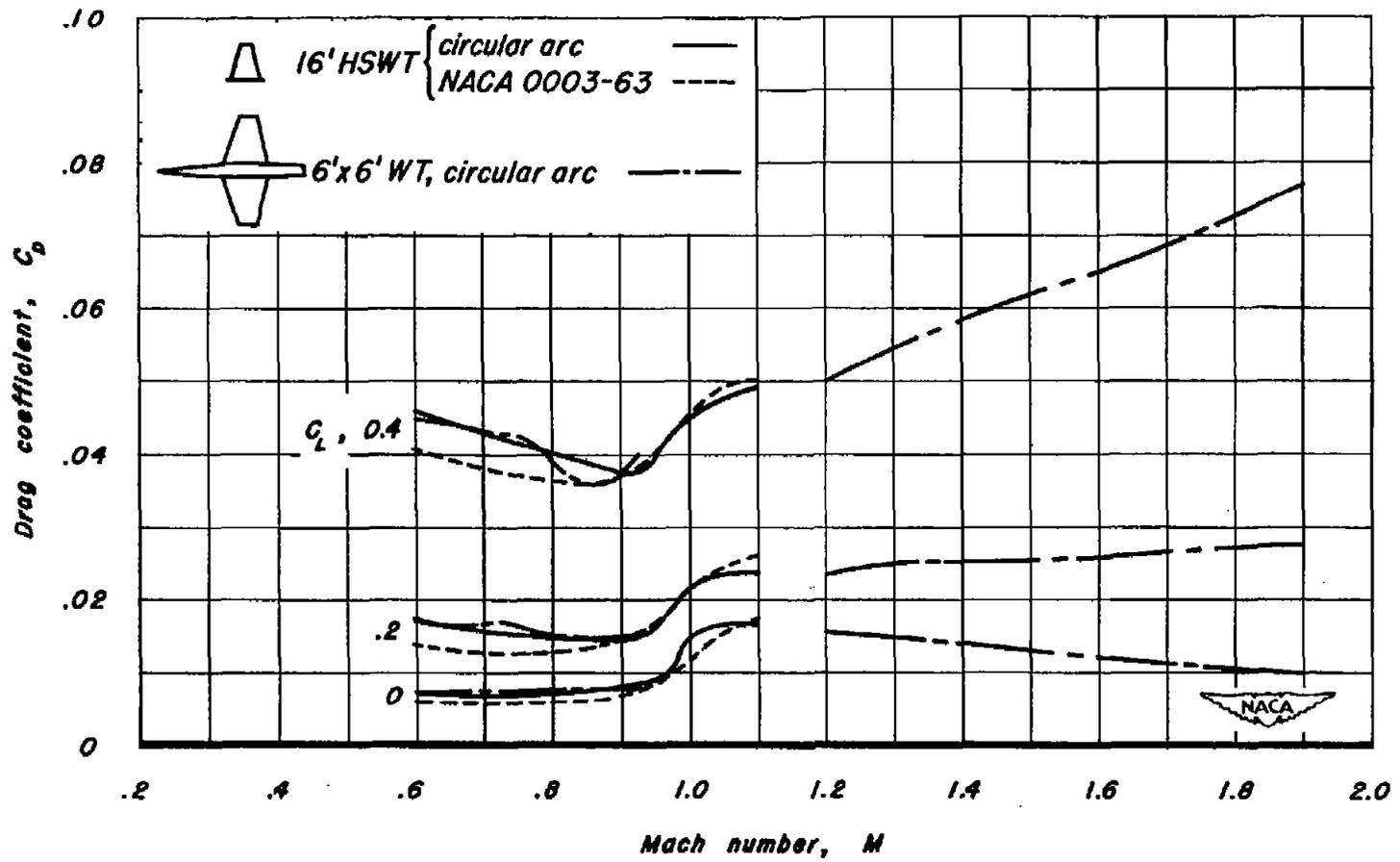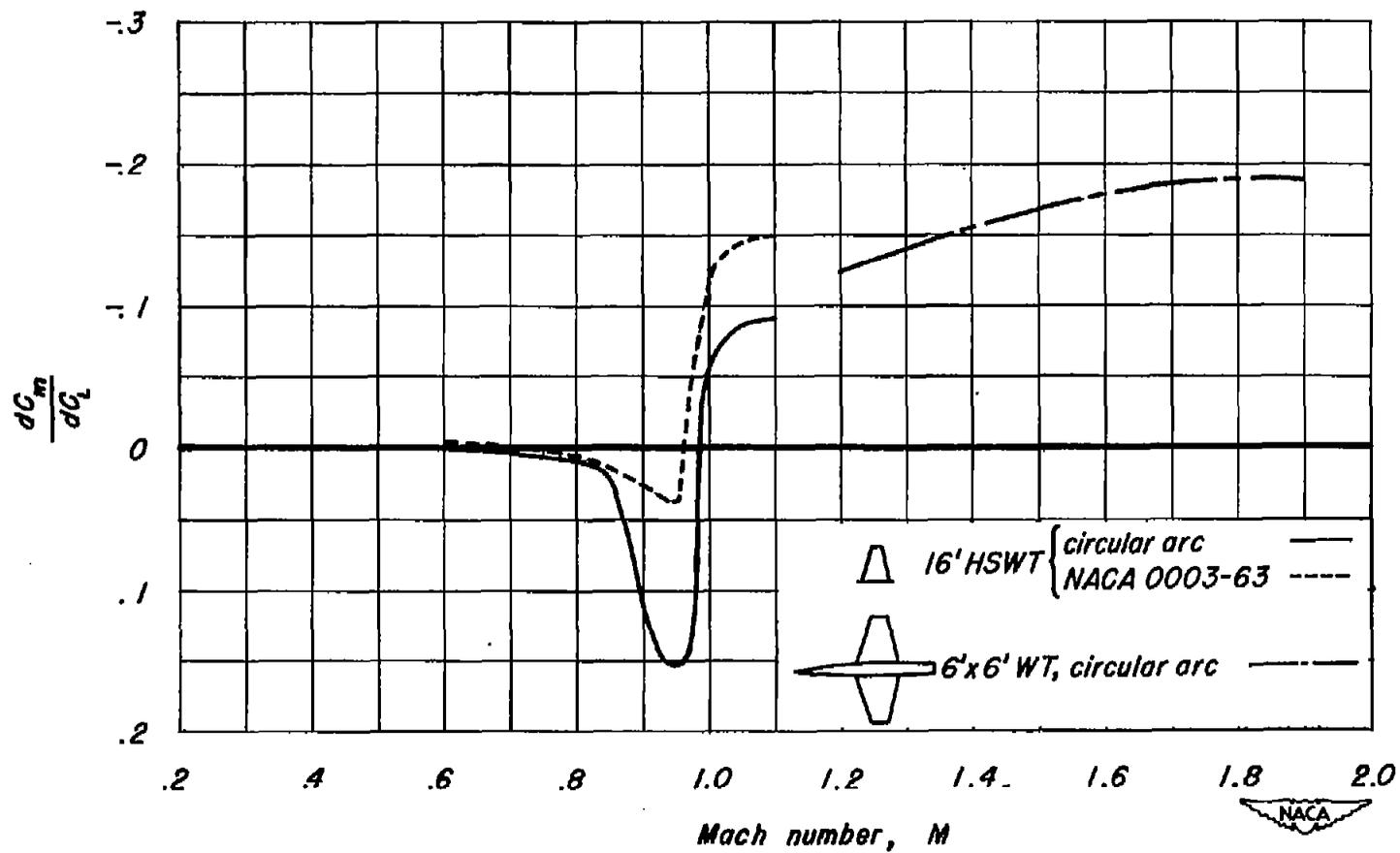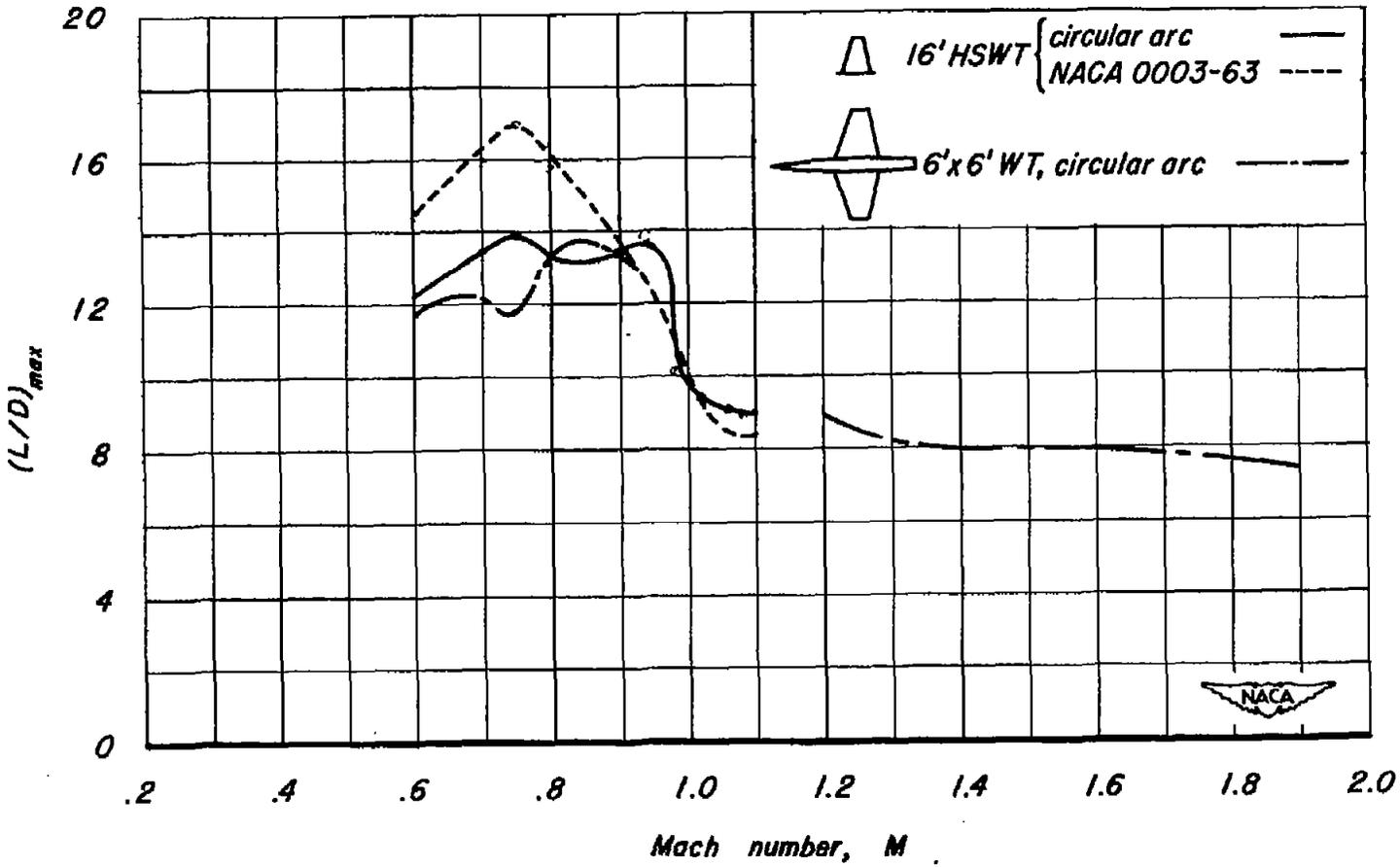Figure 7.— Summary of aerodynamic characteristics as a function of Mach number.
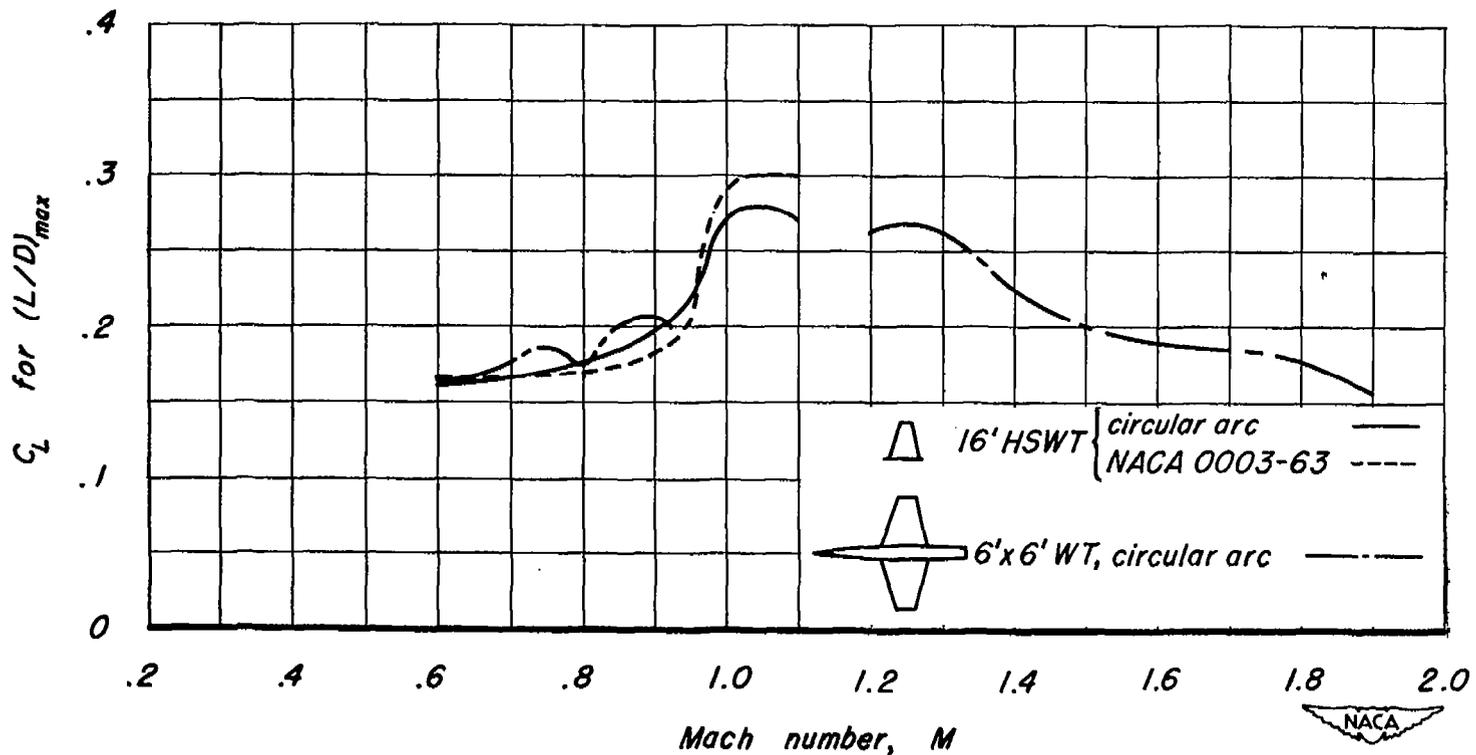
(b) C_D vs M

Figure 7.—Continued.

(c) $\dfrac{dC_m}{dC_L}$ vs M

Figure 7.—Continued.

(d) $(L/D)_{max}$ vs M

Figure 7.—Continued.

(e) C_L for $\left(L/D\right)_{max}$ vs M

Figure 7.-Concluded.